https://doi.org/10.48048/tis.2022.5612

Second-Order Slip Effect on MHD Flow and Radiative Heat Transfer through Porous Medium due to an Exponentially Stretching Sheet

Preeti Kaushik[1,*] and Upendra Mishra[2]

[1]*Department of Mathematics, Inderprastha Engineering College, Uttar Pradesh, India*
[2]*Department of Mathematics, Amity University, Rajasthan, India*

([*]Corresponding author's e-mail: pre.kaushik@gmail.com)

Received: 10 April 2021, Revised: 29 June 2021, Accepted: 6 July 2021

Abstract

The magnetohydrodynamic (MHD) boundary layer flow and radiative heat transfer with second-order slip condition are investigated in this paper. The fluid flow is considered towards an exponentially stretching sheet. The effect of magnetic field and thermal conductivity are taken into account. The obtained nonlinear mathematical expression of the flow are transformed into ordinary differential equations by similarity transformation. The coupled higher order nonlinear ordinary differential equations are solved numerically. The solution for velocity and temperature profile against the first and second-order slip parameters are analyzed. Significant changes are observed in skin friction coefficient and Local Nusselt number due to the magnetic parameter. The characteristics of the flow are discussed through graphs for different pertinent parameters. The results designate that the Local Nusselt number reduces with the increased value of magnetic parameter but opposite behavior is observed for the skin friction coefficient. The rate of heat transfer decreases with higher value of Prandtl number and enhances for Radiation parameter.

Keywords: Exponentially stretching sheet, MHD flow, Second-order slip condition, Heat transfer

Nomenclature

c_p	Specific heat
T	Fluid temperature
T_w	Temperature at wall,
T_∞	Ambient temperature
k	Permeability for Porous medium
k_f	Thermal conductivity
q_r	Radiative heat flux
k_n	Knudsen number
λ	Molecular mean free path
L	Characteristic length
a_1 , a_2	Constant
M	Magnetic parameter
R	Radiation parameter
Pr	Prandtl number
N	Thermal slip coefficient
C_f	Skin friction coefficient
Nu_x	Local Nusselt number
Re_x	Reynolds number.

Greek Symbols

ρ	Fluid density
σ	Chemical reaction rate constant,
α	Momentum adaptation coefficient
γ	First order slip parameter
δ	Second order slip parameter

Introduction

The phenomena of boundary layer fluid flow towards an exponentially stretching sheet has acquired attention of many researchers. The concept of exponentially stretching sheet has been applied in many industrial applications in engineering and technology such as glass fiber, paper production, fusing metals in an electric heater, etc. The major advantage of MHD flow is that it allows estimation of cooling rate. The concept of Magnetohydrodynamic flow together with the energy equation of viscous fluid over an exponentially stretching sheet is being utilized for the production of gas turbine, various devices for aircraft and many space vehicles. Crane [1] have initially examined the velocity of boundary layer flow towards the linear stretching sheet problem which is proportional to the distance. Ibrahim [2] investigated the 2D flow of incompressible viscous fluid towards a stretching sheet. Irfan and Farooq [3] studied the 2 dimensional flow of electrically conducting boundary layer fluid problem towards an exponentially stretching sheet. Ishak [4] analyzed the heat transfer rate due to radiation on MHD flow past an exponentially stretching sheet. Majeed *et al.* [5] proposed the phenomenon of heat transfer in the presence of second order slip condition on an exponentially stretching sheet. Mahantesh *et al.* [6] developed the second order slip model and obtained heat transfer rate over a stretching sheet. Ene and Marinca [7] presented incompressible MHD flow of viscous fluid along with radiative effect. Kumar *et al.* [8] described an unsteady boundary layer flow of nanofluid at stagnation point with the effect of Brownian diffusion. Bhattacharyya *et al.* [9]; Bhattacharyya and Layek [10] discussed the slip effect on heat transfer and boundary layer fluid flow. Aurangzaib *et al.* [11] obtained the boundary layer flow of micropolar fluid in the presence of suction and injection. Bhattacharyya *et al.* [12] discussed the influence of thermal radiation on Casson fluid flow and also examined the heat and mass transfer due to stretching shrinking sheet. Mukhopadhyay [13] investigated the velocity and thermal slip effect on an incompressible viscous fluid flow due to exponentially stretching sheet in the porous medium. Waini *et al.* [14] observed mixed convection nanofluid flow past an exponentially stretching and shrinking surface with suction effect. Nadeem *et al.* [15] presented the impact of Bio-convection slip of 2D micropolar fluid flow due to exponentially stretching surface. Reddy *et al.* [16] discussed magneto hydrodynamic flow of micropolar fluid in the presence of chemical reaction and thermal radiation. Mabood *et al.* [17] addressed the boundary layer flow of viscous fluid at the stagnation point. Nandeppanavar *et al.* [18] studied 2 dimensional boundary layer flow of non-Newtonian fluid in the presence of thermophoresis and Brownian motion. Bhattacharyya and Layek [19]; Bhattacharyya *et al.* [20]; Bhattacharyya *et al.* [21] studied the boundary layer fluid flow over a permeable stretching sheet. Mandal *et al.* [22] discussed heat transfer of the steady boundary layer flow of micropolar fluid. Mabood and Das [23] analyzed the rate of heat transfer of nanofluid flow under the influence of thermal radiation. Ghosh and Mukhopadhyay [24] investigated 2 dimensional steady flow of nanofluid due to exponentially shrinking sheet. Adegbie *et al.* [25] found the effect of thermal conductivity on fluid flow past a stretching sheet. Sheikholeslami and Ganji [26] compared the numerical solution of heat transfer analysis due to porous medium. Many researchers [27-31] investigated the MHD flow over the Newtonian and Non-Newtonian fluid. Zeeshan *et al.* [32] examined the impact of magnetic field and chemical reaction on the nanofluid flow. Xun *et al.* [33] inspected Bio-convection model of viscous fluid flow around rotating plate. Raju *et al.* [34] explored the effect of viscous dissipation and low magnetic field on MHD Cassion fluid flow. Tlili *et al.* [35] analyzed heat and mass transfer of free convection fluid flow due to permeable stretching sheet. Shahzad *et al.* [36] applied the magnetic field to evaluate the rate of heat transfer of axisymmetric Newtonian fluid flow. Mabood *et al.* [37] obtained the numerical solution of the electrically conducting boundary layer fluid problem. Pal and Mandal [38] analyzed the effect of chemical reaction on an incompressible non-newtonian fluid flow over an exponentially stretching sheet. Bhatti *et al.* [39] presented the MHD stagnation point flow and heat transfer past a porous medium. Khalili *et al.* [40] illustrated the radiation effect on the heat and mass transfer of nanofluid flow. Sajid *et al.* [41] obtained the results of nanofluid flow problem by numerical method. Kumar *et al.* [42] investigated Cattaneo-Christov model of Carreau fluid flow towards the stagnation point. Sandhya *et al.* [43] discussed the incompressible fluid flow with the effect of a chemical reaction and magnetic field. Ishak [44] examined the 2 dimensional viscous fluid flow due to the stretching sheet. Bhattacharyya [45] studied the 2-dimensional fluid flow at stagnation point. Mukhopadhyay *et al.* [46] explored the effect of Casson parameter on heat transfer past a stretching sheet.

The purpose of this investigation is to examine the effect of second order slip on MHD flow over an exponentially stretching sheet. The effect of first and second order slip, magnetic parameter, radiation parameter explored in this study. The study offers important insights into the boundary layer flow problems in a porous medium. The mathematical equations are solved numerically by bvp4c through Matlab. The fluid velocity and temperature profile for pertinent parameters are presented graphically. The results validate with the previously published work and found to be in good agreement.

Mathematical formulation

We are considering 2-dimensional magnetohydrodynamic fluid flow towards an exponentially stretching sheet. The stretching sheet is taken along x axis at $y = 0$. A strong magnetic field of strength B_0 applied, where B_0 is constant and it is applied normal to the x axis. The induced magnetic field is not taken into account because of the low value of the Reynolds number. Here it is considered that thermal conductivity varies linear with temperature. $u_w = -Ce^{x/L}$ is velocity at boundary, where C is constant, $v = v_w = v_0 e^{x/2L}$ is a special kind of velocity, where v_0 is a constant, v_0 is considered as velocity suction for $v(x) > 0$, when $v(x) < 0$, v_0 is the velocity blowing, $T = T_w = T_\infty + T_0 e^{x/2L} + N\frac{\partial T}{\partial y}$ is fluid temperature. T_w is fluid temperature at wall, $T_\infty$is ambient temperature, T_0 is reference temperature, N is thermal slip coefficient. The governing equations of continuity, momentum and energy for boundary layer flow problems are represented as [41,42].

$$\frac{\partial u}{\partial x} + \frac{\partial v}{\partial y} = 0 \tag{1}$$

$$u\frac{\partial u}{\partial x} + v\frac{\partial v}{\partial x} = \nu\frac{\partial^2 u}{\partial y^2} - \frac{\nu u}{k} - \frac{\sigma B^2}{\rho}u \tag{2}$$

$$\rho c_p\left[u\frac{\partial T}{\partial x} + v\frac{\partial T}{\partial y}\right] = k_0\frac{\partial^2 T}{\partial y^2} - \frac{\partial q_r}{\partial y} \tag{3}$$

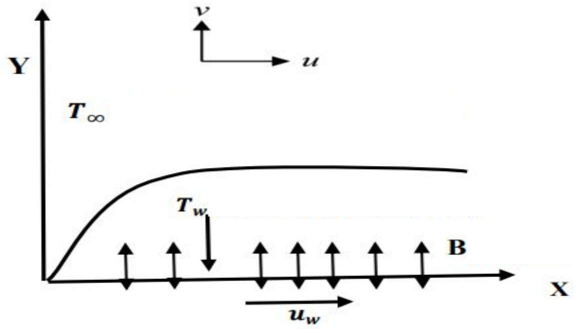

Figure 1 Physical model of the flow.

where u and v are fluid velocity components along x and y axis respectively. ν is kinematic viscosity, k is permeability for Porous medium, ρ is fluid density, σ is chemical reaction rate constant, c_p is specific heat, T is fluid temperature, k_f is thermal conductivity, q_r is radiative heat flux, $B = B_0 e^{x/2L}$ is magnetic field where B_0 is magnetic field constant.

The corresponding boundary conditions are:

$$u_w = -Ce^{x/L} \tag{4}$$

$$u_{slip} = \frac{2}{3}\left(\frac{3-\alpha l^3}{\alpha} - \frac{2}{3}\frac{1-l^2}{k_n}\right)\lambda\frac{\partial u}{\partial y} - \frac{1}{4}\left(l^4 + \frac{2}{k_n^2}(1-l^2)\right)\lambda^2\frac{\partial^2 u}{\partial y^2} = a_1\frac{\partial u}{\partial y} + a_2\frac{\partial^2 u}{\partial y^2} \tag{5}$$

$$u = u_w + u_{slip} = -Ce^{x/L} + a_1\frac{\partial u}{\partial y} + a_2\frac{\partial^2 u}{\partial y^2} \tag{6}$$

$$v = v_w = v_0 e^{x/2L}, T = T_w = T_\infty + T_0 e^{x/2L} + N\frac{\partial T}{\partial y} \quad \text{at } y = 0 \tag{7}$$

$$u \to 0,\ T \to T_\infty \text{ at } y \to \infty \tag{8}$$

k_n is Knudsen number,α is momentum adaptation coefficient, λ is molecular mean free path. $l = \min\left[\frac{1}{k_n}, 1\right]$, L is characteristic length. a_1 and a_2 are constant.

Similarity transformation

Taking similarity transformation by using stream function $\psi(x, y)$;

$$u = \frac{\partial\psi}{\partial y}, v = -\frac{\partial\psi}{\partial x} \tag{9}$$

The stream function uniformly satisfies Eqs. (1) - (2) reduced to

$$\frac{\partial\psi}{\partial y}\cdot\frac{\partial^2\psi}{\partial y\partial x} - \frac{\partial\psi}{\partial x}\frac{\partial^2\psi}{\partial y^2} - \nu\frac{\partial^3\psi}{\partial y^3} - \frac{\sigma B^2}{\rho}\frac{\partial\psi}{\partial y} \tag{10}$$

where $B = B_0 e^{x/2L}$.

Using Rosseland approximation. $q_r = -\frac{4\sigma}{3k^*}\frac{\partial T^4}{\partial y}$, T^4 is linear temperature function, where k^* is mean absorption coefficient, σ is Stefan Boltzman constant, the function T^4 expanded in Taylor's series and ignoring the higher terms. We have $T^4 = 4T_\infty^3 T - 3T_\infty^4$. Therefore Eq. (3) becomes;

$$\rho c_p\left[u\frac{\partial T}{\partial x} + v\frac{\partial T}{\partial y}\right] = k_0\frac{\partial^2 T}{\partial y^2} - \frac{16\sigma T_\infty^3}{3k^*}\frac{\partial^2 T}{\partial y^2} \tag{11}$$

Using stream function Eq. (11) becomes;

$$\rho c_p\left[\frac{\partial\psi}{\partial y}\frac{\partial T}{\partial x} - \frac{\partial\psi}{\partial x}\frac{\partial T}{\partial y}\right] = k_0\frac{\partial^2 T}{\partial y^2} - \frac{16\sigma T_\infty^3}{3k^*}\frac{\partial^2 T}{\partial y^2} \tag{12}$$

where

$$\psi = \sqrt{2\nu LC}.\mathrm{f}(\eta)e^{x/2L},\ \eta = y\sqrt{\frac{C}{2\nu L}}e^{x/2L},\ \theta = \frac{T-T_\infty}{T_w-T_\infty}, \tag{13}$$

For the similarity solution permeability is assumed to have the following form

$$k(x) = 2k_0 e^{-x/L} \tag{14}$$

where k_0 is reference permeability.

The Thermal conductivity of the fluid varies linearly with temperature.

$$k_f = k_\infty(1 + \epsilon\theta) \tag{15}$$

where ϵ is thermal conductivity variation parameter.

Using similarity transformation and boundary layer approximation Eqs. (10) - (12) become;

$$f''' + ff'' - 2f'^2 - \frac{f'}{K} - Mf' = 0 \tag{16}$$

$$(1 + \frac{4}{3}R)\,\theta'' + \Pr(f\,\theta' - f'\,\theta) = 0 \tag{17}$$

With boundary conditions

$$f'(0) = 1 + \gamma f''(0) + \delta f'''(0), f(0) = S, \theta(0) = 1 + \alpha^* \theta'(0) \quad as\ \eta = 0 \tag{18}$$

$$f'(\eta) \to 0\,, \theta(\eta) \to 0 \qquad as\ \eta \to \infty \tag{19}$$

where $M = \frac{2\sigma B_0^2 L}{\rho C}$ is magnetic parameter,$R = \frac{4\sigma T_\infty^3 L}{kk^*}$ is radiation parameter, $Pr = \frac{\rho C_p}{k_\infty}$ prandtl number, $\gamma = a_1 \sqrt{\frac{C}{2vL}} e^{x/2L}$ is first order slip parameter and $\delta = a_2 \left(\frac{C}{2vL} e^{x/L}\right)$ is second order slip parameter. $\alpha^* = N \sqrt{\frac{C}{2vL}} e^{x/2L}$ is thermal slip parameter.

The physical quantities of interest are Skin friction coefficient and Nusselt number, we get from above equations

$$C_f = \frac{\tau_w}{\rho u_w^2} \quad \text{where the wall shear stress} \quad \tau_w = \mu \left(\frac{\partial u}{\partial y}\right)_{y=0} \tag{20}$$

$$Nu_x = \frac{x q_w}{k(T_w - T_\infty)} \quad \text{where the wall heat flux} \quad q_w = -R\left(\frac{\partial T}{\partial y}\right)_{y=0} \tag{21}$$

$$C_f = \sqrt{\frac{x}{2L}} Re_x^{-1/2} f''(0)\,, Nu_x = -\sqrt{\frac{x}{2L}} Re_x^{-1/2} \theta'(0) \tag{22}$$

where $Re_x = \frac{u_w x}{v}$ represents the Reynolds number.

Numerical solution

The highly nonlinear system of ordinary differential Eqs. (16) - (17) with the corresponding boundary conditions (18) and (19) are solved numerically using MATLAB bvp4c software. The software is using finite difference method to solve the boundary value problems. The transformed equations converted into initial value problem by taking the following transformation.

$$f' = z\,,\ z' = p, \quad p' = Mz + \frac{z}{K} + 2z^2 - fp \tag{23}$$

$$\theta' = q \quad q' = -\frac{pr(fq - z\theta)}{(1 + \frac{4}{3}R)}$$

and the transformed dimensionless boundary conditions becomes;

$$f(0) = S, (0) = 1 + \gamma p(0) + \delta p'(0)\,, \theta(0) = 1 + \alpha q(0). \tag{24}$$

$$z(\infty) = 0, \theta(\infty) = 0.$$

Finite value for boundary condition $\eta \to \infty$, i.e. η_{max} taken as 40. The step size is taken as $\nabla\eta = 0.01$, with the tolerance limit up to 10^{-5}. Trial values of $f''(0), \theta'(0)$ were adjusted to get a better approximation to satisfy the corresponding boundary condition.

Results and discussion

The study has been performed for the 2-dimensional flow pattern. The dimensionless quantities velocity and temperature profile are present in graphical and tabular form for different parameters. The numerical solution has been obtained for transformed Eqs. (16) - (17) with boundary conditions Eqs. (18) - (19). Boundary layer flow and heat transfer has been represented through graphs for different pertinent parameter first-order slip parameter (γ), second-order slip parameter (δ), magnetic parameter (M) and Prandtl number (Pr). The non-dimensional values $\gamma = 0,\ \delta = -1,\ M = 0.2,\ R = 0.7,\ Pr = 0.5,\ \alpha = -2$ are taken commonly in the complete investigation.

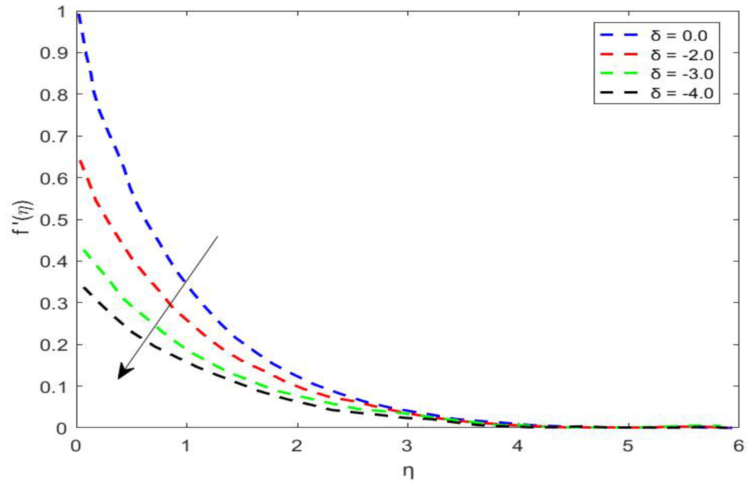

Figure 2 Variation of $f'(\eta)$ for the different values of δ for $\gamma = 0,\ M = 0.2,\ R = 0.7,\ Pr = 0.5,\ \alpha = -2$.

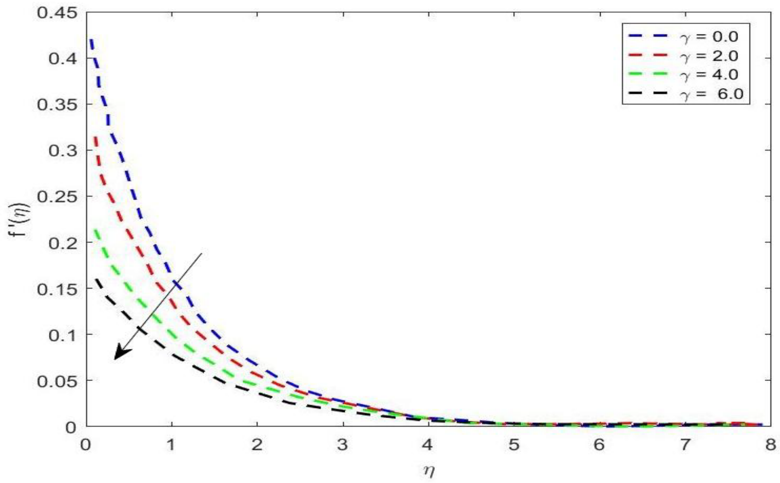

Figure 3 Variation of $f'(\eta)$ for the different values of γ for $\delta = -1,\ M = 0.2,\ R = 0.7,\ Pr = 0.5,$ $\alpha = -2$.

Figure 2 illustrate the Impact of second-order slip parameter (δ) on velocity profile$f'(\eta)$. The result engrossing to notice that velocity slowly decreasing when the value of second-order slip parameter (δ) increases. **Figure 3** depicts the influence of first-order slip parameter (γ) on velocity profile $f'(\eta)$, the results elaborate that velocity profile $f'(\eta)$ decays for the increasing value of first order slip parameter (γ). The first order slip parameter (γ) and second-order slip parameter (δ) enhances the resistance of fluid flow that causes the decreasing of the velocity profile $f'(\eta)$.

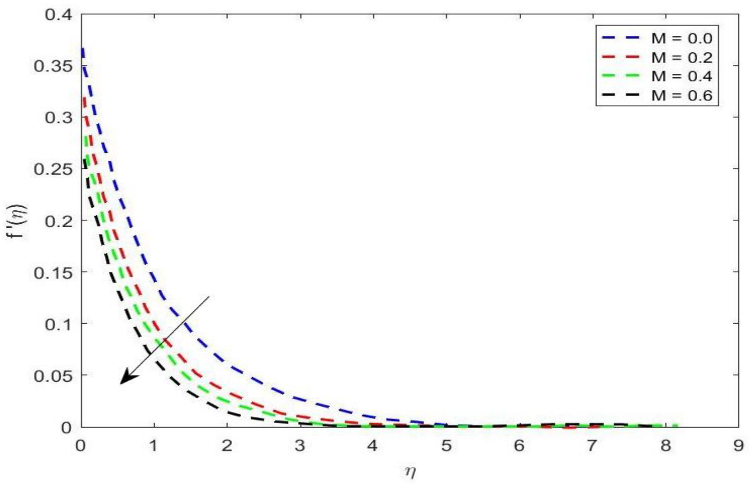

Figure 4 Variation of $f'(\eta)$ for the different values of M for values $\gamma = 0,\ \delta = -1,\ R = 0.7,\ Pr = 0.5,\ \alpha = -2$.

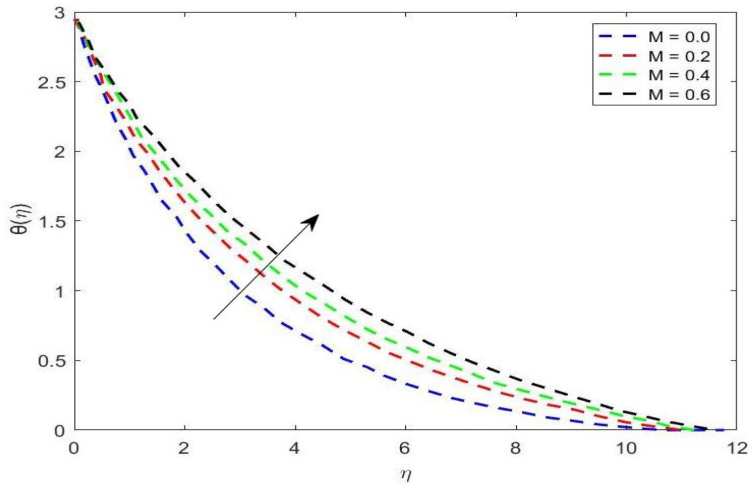

Figure 5 Variation of $\theta(\eta)$ for the different values of M for $\gamma = 0,\ \delta = -1,\ R = 0.7,\ Pr = 0.5,\ \alpha = -2$.

Figure 4 represents the behavior of the velocity profile $f'(\eta)$ due to magnetic parameter (M). The graph clearly described that velocity profile $f'(\eta)$ reduces due to high magnetic parameter M. For $M = 0$ fluid flow considered as hydrodynamic flow although $M \neq 0$ is considered as hydro-magnetic flow. The velocity of the fluid is released as *M* increases. The effect of a physical magnetic field creates a resistive force that causes resistance. It has the ability to slow the movement of the fluid. **Figure 5** provides the variation in the temperature profile $\theta(\eta)$, for different values of magnetic parameter M. It is observed that temperature profile $\theta(\eta)$ is increasing function for the large magnetic parameter M. It is also observed that the temperature of the fluid is higher for hydro-magnetic flow.

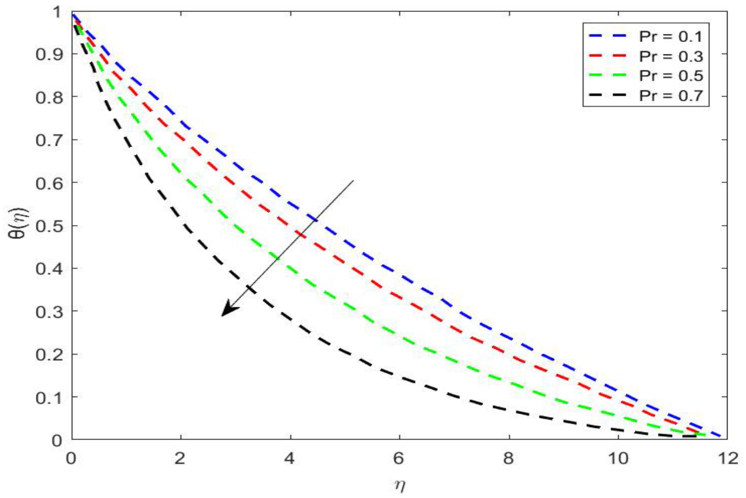

Figure 6 Variation of $\theta(\eta)$ for the different values of Pr for $\gamma = 0,\ \delta = -1,\ M = 0.2,\ R = 0.7,\ \alpha = -2$.

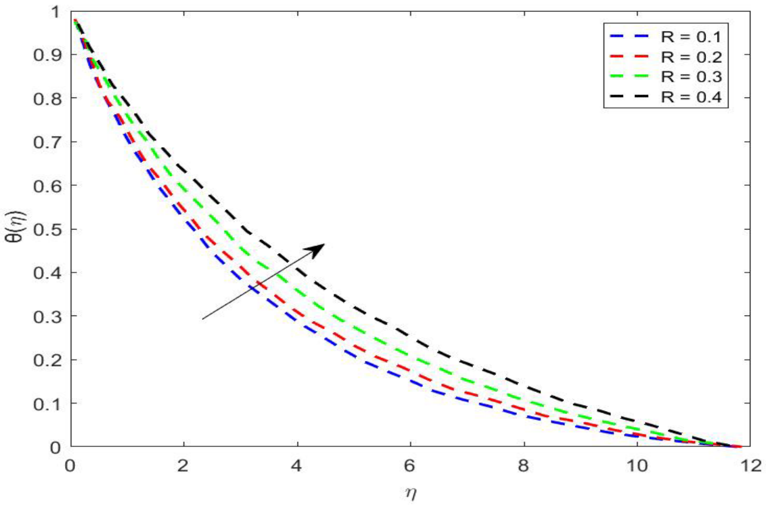

Figure 7 Variation of $\theta(\eta)$ for the different values of R for $\gamma = 0$, $\delta = -1,\ M = 0.2,\ Pr = 0.5,\ \alpha = -2$.

Figure 6 demonstrate the effect of Prandtl number (Pr) on temperature profile $\theta(\eta)$. The graph elucidate that temperature profile $\theta(\eta)$ gradually decreases with the increasing value of Prandtl number (Pr)**.** It is due to the property of Prandtl number that momentum diffusivity is higher than thermal diffusivity for large vale of Pr**. Figure 7** shows that the impact of Radiation parameter (R) on temperature profile $\theta(\eta)$. Graph elaborate that temperature profile $\theta(\eta)$ enhances against the Radiation parameter (R)**.** Due to the phenomenon of electromagnetic radiation, Thermal energy generates in the fluid flow because of radiation parameter. That causes to increase in the temperature profile.

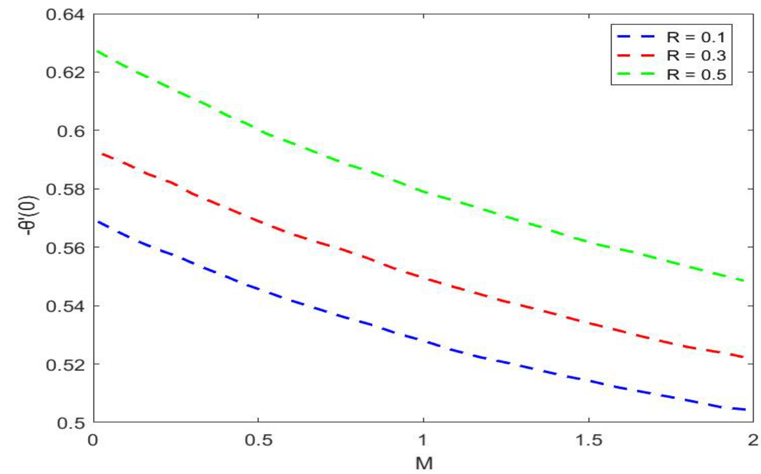

Figure 8 Variation of $\theta'(0)$ for the different values of R for $\gamma = 0,\ \delta = -1,\ M = 0.2,\ Pr = 0.5,\ \alpha = -2$.

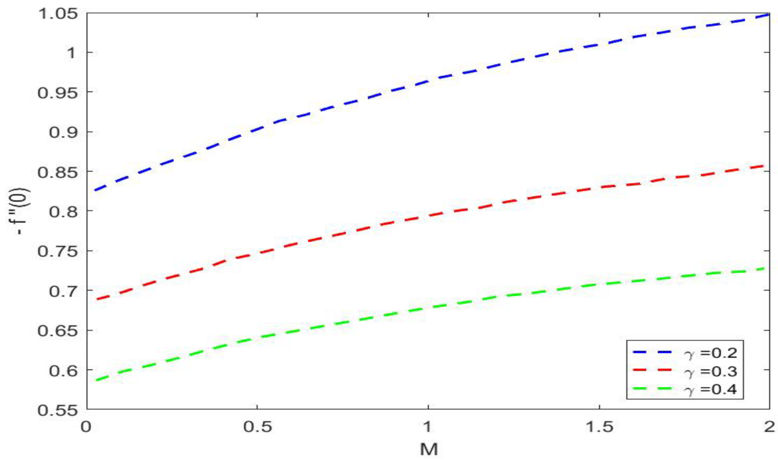

Figure 9 Variation of $f''^{(0)}$ for the different values of γ for $\delta = -1,\ M = 0.2,\ R = 0.7,\ Pr = 0.5,$ $\alpha = -2$.

Figure 8 plotted to observe the effect of different magnetic parameter (M) and Radiation parameter (R) on Nusselt number $\theta'(0)$**.** The Nusselt number graph reduces as the absolute value of the magnetic parameter (M) and Radiation parameter (R) increases. **Figure 9** visualize the effect of magnetic parameter (M) and first-order slip parameter (γ) on the skin friction coefficient $f''(0)$. The graph shows that skin friction coefficient $f''(0)$ rises up for the large value of magnetic parameter M and first-order slip parameter γ. To validate the results and accuracy of the method used data compared with previously published literature. Furthermore **Table 1** displays the Local Nusselt number $-\theta'(0)$ for different values of Prandtl number. Obtained results are found excellent consistency found with published results in Sandhya *et al.* [43].

Table 1 Comparison study for the values of Nusselt number – $\theta'^{(0)}$ with magnetic field M when $\gamma = 0$, $\delta = -1, M = 0.2, R = 0.7, \alpha = -2$.

Pr	**Sandhya *et al.* [43]**	**Ishak [44]**	**Present result**
1	0.954784	0.9548	0.95478392
3	1.869073	1.8691	1.86907423
4	2.204507	2.5001	2.20450691

Conclusions

In this study, we investigated the impact of second-order velocity slip condition on the 2-dimensional flow of the fluid towards an exponentially stretching sheet. The effect of pertinent parameters on the velocity profile and temperature profile has been investigated. The major findings are summarized as follows:

1) In comparison to the second-order slip parameter ($\delta = -2$), Velocity profile $f'(\eta)$ is a decreasing function for second-order slip parameter ($\delta = -4$). This is due to an enhancement in resistance of fluid flow, which results in a decrement in the velocity profile $f'(\eta)$.

2) Velocity profile $f'(\eta)$ is maximum for the first order slip parameter ($\gamma = 0$) while it is lower for the first order slip parameter ($\gamma = 6$). This shows a significant decrement in the velocity profile.

3) Velocity profile $f'(\eta)$ is higher for the low magnetic parameter ($M = 0$) but it is lower for high magnetic parameter ($M = 0.6$). This reduction in velocity profile occurs due to the effect of resistive force generated by magnetic field.

4) Temperature profile $\theta(\eta)$ is lesser for magnetic parameter ($M = 0$), but for magnetic parameter ($M = 0.6$), it displays a higher value of temperature profile $\theta(\eta)$. The increasing variation was observed in temperature profile for the magnetic parameter.

5) Temperature profile $\theta(\eta)$ is maximum for Prandtl number ($Pr = 0.1$) but it decreases for Prandtl number ($Pr = 0.7$). The opposite behavior observed in Temperature profile against the Radiation parameter.

6) The local Nusselt number is maximum for Radiation parameter ($R = 0.1$) but it is minimum for the Radiation parameter ($R = 0.5$). The skin friction coefficient was observed minimum for first-order slip parameter ($\gamma = 0.2$), whereas it is maximum for first-order slip parameter ($\gamma = 0.4$). This shows that the local Nusselt number reduces for rising values of Radiation parameter while the skin friction coefficient increases for the higher value of first-order slip parameter.

References

[1] LJ Crane. Flow past a stretching plate. *ZAAM J. Appl. Math. Phys.* 1970; **21**, 645-7.

[2] W Ibrahim. Magnetohydrodynamics (MHD) flow of a tangent hyperbolic fluid with nanoparticles past a stretching sheet with second order slip and convective boundary condition. *Results Phys.* 2017; **7**, 3723-31.

[3] M Irfan and MA Farooq. Thermophoretic MHD free stream flow with variable internal heat generation/ absorption and variable liquid characteristics in a permeable medium over a radiative exponentially stretching sheet. *J. Mater. Res. Tech.* 2020; **9**, 4855-66.

[4] A Ishak. MHD boundary layer flow due to an exponentially stretching sheet with radiation effect. *Sains Malaysiana* 2011; **40**, 391-5.

[5] A Majeed, FM Noori, A Zeeshan, T Mahmood, SU Rehman and I Khan. Analysis of activation energy in magnetohydrodynamic flow with chemical reaction and second order momentum slip model. *Case Stud. Therm. Eng.* 2018; **12**, 765-73.

[6] MM Nandeppanavar, K Vajravelu, MS Abel and MN Siddalingapp. Second order slip flow and heat transfer over a stretching sheet with non-linear Navier boundary condition. *Int. J. Therm. Sci.* 2012; **58**, 143-50.

[7] RD Ene and V Marinca. Approximate solutions for steady boundary layer MHD viscous flow and radiative heat transfer over an exponentially porous stretching sheet. *Appl. Math. Comput.* 2015; **269**, 389-401.

[8] R Kumar, S Sood, SA Shehzad and M Sheikholeslami. Numerical modeling of time-dependent bio-convective stagnation flow of a nanofluid in slip regime. *Results Phys*. 2017; **7**, 3325-32.

[9] K Bhattacharyya, S Mukhopadhyay and GC Layek. Slip effects on an unsteady boundary layer stagnation-point flow and heat transfer towards a stretching sheet. *Chin. Phys. Lett.* 2011; **28**, 094702.

[10] K Bhattacharyya and GC Layek. Slip effect on diffusion of chemically reactive species in boundary layer flow over a vertical stretching sheet with suction or blowing. *Chem. Eng. Comm.* 2011; **198**, 1354-65.

[11] Aurangzaib, MS Uddin, K Bhattacharyya and S Shafie. Micropolar fluid flow and heat transfer over an exponentially permeable shrinking sheet. *Propul. Power Res.* 2016; **5**, 310-7.

[12] K Bhattacharyya, MS Uddin and GC Layek. Exact solution for thermal boundary layer in Casson fluid flow over permeable shrinking sheet with variable wall temperature and thermal radiation. *Alexandria Eng. J.* 2016; **55**, 1703-12.

[13] S Mukhopadhyay. Slip effects on MHD boundary layer flow over an exponentially stretching sheet with suction/blowing and thermal radiation. *Ain Shams Eng. J.* 2013; **4**, 485-91.

[14] I Waini, A Ishak and I Pop. Mixed convection flow over an exponentially stretching/shrinking vertical surface in a hybrid nanofluid. *Alexandria Eng. J.* 2020; **59**, 1881-91.

[15] S Nadeem, MN Khan and N Abbas. Transportation of slip effects on nanomaterial micropolar fluid flow over exponentially stretching. *Alexandria Eng. J.* 2020; **59**, 3443-50.

[16] NN Reddy, VS Rao and BR Reddy. Chemical reaction impact on MHD natural convection flow through porous medium past an exponentially stretching sheet in presence of heat source/sink and viscous dissipation. *Case Stud. Therm. Eng.* 2021; **25**, 100879.

[17] F Mabood, A Shafiq, T Hayat and S Abelman. Radiation effects on stagnation point flow with melting heat transfer and second order slip. *Results Phys.* 2017; **7**, 31-42.

[18] MM Nandeppanavar, S Vaishali, MC Kemparaju and N Raveendra. Theoretical analysis of thermal characteristics of Casson nano fluid flow past an exponential stretching sheet in Darcy porous media. *Case Stud. Therm. Eng*. 2020; **21**, 100717.

[19] K Bhattacharyya and GC Layek. Chemically reactive solute distribution in MHD boundary layer flow over a permeable stretching sheet with suction or blowing. *Chem. Eng. Comm.* 2010; **197**, 1527-40.

[20] K Bhattacharyya, S Mukhopadhyay and GC Layek. Unsteady MHD boundary layer flow with diffusion and first-order chemical reaction over a permeable stretching sheet with suction or blowing. *Chem. Eng. Comm*. 2013; **200**, 379-97.

[21] K Bhattacharyya, T Hayat and A Alsaedi. Exact solution for boundary layer flow of Casson fluid over a permeable stretching/shrinking sheet. *ZAMM J. Appl. Math. Mech*. 2014; **94**, 522-8.

[22] IC Mandal and S Mukhopadhyay. Nonlinear convection in micropolar fluid flow past an exponentially stretching sheet in an exponentially moving stream with thermal radiation. *Mech. Adv. Mate. Struct.* 2019; **26**, 2040-6.

[23] F Mabood and K Das. Melting heat transfer on hydromagnetic flow of a nanofluid over a stretching sheet with radiation and second-order slip. *Eur. Phys. J. Plus* 2016; **131**, 3.

[24] S Ghosh and S Mukhopadhyay. Flow and heat transfer of nanofluid over an exponentially shrinking porous sheet with heat and mass fluxes. *Propul. Power Res.* 2018; **7**, 268-75.

[25] SK Adegbie, OK Koriko and IL Animasaun. Melting heat transfer effects on stagnation point flow of micropolar fluid with variable dynamic viscosity and thermal conductivity at constant vortex viscosity. *J. Nigerian Math. Soc*. 2016; **35**, 34-47.

[26] M Sheikholeslami and DD Ganji. Nanofluid convective heat transfer using semi analytical and numerical approaches: A review. *J. Taiwan Inst. Chem. Eng.* 2016; **65**, 43-77.

[27] K Bhattacharyya and GC Layek. Magnetohydrodynamic boundary layer flow of nanofluid over an exponentially stretching permeable sheet. *Phys. Res. Int.* 2014; **2014**, 592536.

[28] I Ullah, K Bhattacharyya, S shafie and I Khan. Unsteady MHD mixed convection slip flow of Casson fluid over nonlinearly stretching sheet embedded in a porous medium with chemical reaction, thermal radiation, heat generation/absorption and convective boundary conditions. *Plos One* 2016; **11**, e0165348.

[29] GS Seth, AK Singha, MS Mandal, A Banerjee and K Bhattacharyya. MHD stagnation-point flow and heat transfer past a non-isothermal shrinking/stretching sheet in porous medium with heat sink or source effect. *Int. J. Mech. Sci*. 2017; **134**, 98-111.

[30] K Bhattacharyya, S Mukhopadhyay and GC Layek. Reactive solute transfer in magnetohydrodynamic boundary layer stagnation-point flow over a stretching sheet with suction/blowing. *Chem. Eng. Comm*. 2012; **199**, 368-83.

[31] B Mandal, K Bhattacharyya, A Banerjee, AK Verma and AK Gautam. MHD mixed convection on an inclined stretching plate in Darcy porous medium with Soret effect and variable surface conditions. *J. Nonlinear Eng*. 2020; **9**, 457-69.

[32] A Zeeshan, N Shehzad and R Ellahi. Analysis of activation energy in Couette-Poiseuille flow of nanofluid in the presence of chemical reaction and convective boundary conditions. *Results Phys.* 2018; **8**, 502-12.

[33] S Xun, J Zhao, L Zheng and X Zhang. Bioconvection in rotating system immersed in nanofluid with temperature dependent viscosity and thermal conductivity. *Int. J. Heat Mass Tran*. 2017; **111**, 1001-6.

[34] CSK Raju, N Sandeep, V Sugunamma, MJ Babu and JVR Reddy. Heat and mass transfer in magnetohydrodynamic Casson fluid over an exponentially permeable stretching surface. *Eng. Sci. Tech. Int. J.* 2016; **19**, 45-52.

[35] I Tlili, MM Bhatti, SM Hamad, AA Barzinjy, M Sheikholeslami and A Shafee. Macroscopic modeling for convection of Hybrid nanofluid with magnetic effects. *Stat. Mech. Appl*. 2019; **534**, 122136.
[36] A Shahzad, R Ali, M Kamran, SUD Khan, SUD Khan and A Farooq. Axisymmetric flow with heat transfer over exponentially stretching sheet: A computational approach. *Stat. Mech. Appl.* 2020; **554**, 124242.
[37] F Mabood, WA Khan and AIM Ismail. MHD flow over exponential radiating stretching sheet using homotopy analysis method. *J. King Saud Univ. Eng. Sci*. 2017; **29**, 68-74.
[38] D Pal and G Mandal. Double diffusive magnetohydrodynamic heat and mass transfer of nanofluids over a nonlinear stretching/shrinking sheet with viscous-Ohmic dissipation and thermal radiation. *Propul. Power Res*. 2017; **6**, 58-69.
[39] MM Bhatti, T Abbas and MM Rashidi. A new numerical simulation of MHD stagnation-point flow over a permeable stretching/shrinking sheet in porous media with heat transfer. *Iranian J. Sci. Tech. Trans. A Sci*. 2017; **41**, 779-85.
[40] NNW Khalili, AA Samson, ASA Aziz and ZM Ali. Chemical reaction and radiation effects on MHD flow past an exponentially stretching sheet with heat sink. *J. Phys. Conf. Ser.* 2017; **890**, 012025.
[41] T Sajid, M Sagheer, S Hissain and M Bilal. Darcy-Forchheimer flow of Maxwell nanofluid flow with nonlinear thermal radiation and activation energy. *AIP Adv*. 2018; **8**, 035102.
[42] RK Kumar, GV Kumar, CSK Raju, SA Shehzad and SVK Varma. Analysis of Arrhenius activation energy in magnetohydrodynamic Carreau fluid flow through improved theory of heat and binary chemical reaction. *J. Phys. Comm*. 2018; **2**, 035004.
[43] G Sandhya, G Sarojamma, PVS Narayana and B Venkateswarlu. Buoyancy forces and activation energy on the MHD radiative flow over an exponential stretching sheet with second-order slip. *Heat Tran.* 2020; **50**, 784-800.
[44] A Ishak. MHD boundary layer flow due to an exponentially stretching sheet with radiation effect. *Sains Malaysiana* 2011; **40**, 391-5.
[45] K Bhattacharyya. Boundary layer stagnation-point flow of Casson fluid and heat transfer towards a shrinking/stretching sheet. *Front. Heat Mass Tran*. 2013; **4**, 023003.
[46] S Mukhopadhyay, K Bhattacharyya and T Hayat. Exact solutions for the flow of Casson fluid over a stretching surface with transpiration and heat transfer effects. *Chin. Phys. B* 2013; **22**, 114701.